Kinetic Studies with Iodine-123-Labeled Serum Amyloid P Component in Patients with Systemic AA and AL Amyloidosis and Assessment of Clinical Value

Pieter L. Jager, Bouke P.C. Hazenberg, Eric J.F. Franssen, Piet C. Limburg, Martin H. van Rijswijk and D. Albertus Piers
Departments of Nuclear Medicine and Rheumatology, University Hospital Groningen, The Netherlands

In systemic amyloidosis, widespread amyloid deposition interferes with organ function, frequently with fatal consequences. Diagnosis rests on demonstrating amyloid deposits in the tissues, traditionally with histology although scintigraphic imaging with radiolabeled serum amyloid P component (SAP) has lately been developed as a specific noninvasive alternative. We report a detailed analysis of the abnormal turnover of SAP in patients with systemic amyloidosis and an assessment of its clinical value. **Methods:** Iodine-123-labeled human SAP (200 MBq) SAP was injected intravenously into 49 patients with histologically proven systemic AA- or AL- amyloidosis and in 7 control subjects. Plasma clearance and whole-body retention of labeled SAP were analyzed over 48 hr using plasma sampling, whole-body gamma camera imaging and measurement of radioactivity in the urine. The rate of SAP synthesis and interstitial exchange were determined, and the size of the amyloid compartment was compared with clinical estimates of whole-body amyloid load and patient survival. **Results:** All plasma time-activity curves were biphasic. In comparison with control subjects, patients with amyloidosis showed significantly faster plasma disappearance [4-hr value: AA 48% ± 18%, AL 45%±15% versus 65% ± 8% (p < 0.05)], higher total-body retention 48 hr p.i. [AA 74% ± 14%, AL 73% ± 17% versus 46% ± 15% (p < 0.01)] and especially higher extravascular retention 48 hr p.i. [AA 59% ± 16%, AL 58%±19% versus 30% ± 14% (p < 0.01)]. Extravascular retention correlated with clinical estimation of the amyloid load. If extravascular retention values in patients with AL amyloidosis were over 60%, survival was decreased (median 4 versus 23 mo, p < 0.001). Markedly increased interstitial exchange rates were present in amyloidosis (AA 64 ± 61, AL 50 ± 37 versus 18 ± 8 mg/hr), whereas the SAP synthesis rate did not differ from the control values (AA 5.0 ± 3.0, AL 5.5 ± 3.2 versus 4.5 ± 1.4 mg/hr). **Conclusion:** The presence of systemic amyloidosis is characterized by accelerated initial clearance of ^{123}I-SAP from the plasma and increased interstitial exchange rate and extravascular retention. These findings reflect reversible binding of radiolabeled SAP to amyloid deposits and provide clinically useful information for diagnosis, monitoring of therapy and prognosis in patients with systemic amyloidosis.

Key Words: amyloidosis; serum amyloid P component; diagnosis; iodine-123

J Nucl Med 1998; 39:699–706

Amyloidosis is a serious condition caused by deposition of fibrillar protein, amyloid, in various tissues leading to severe organ dysfunction and eventually death (*1*). There are many different subtypes that can be characterized by systemic or localized deposition of amyloid and by different amyloid fibril precursor proteins in plasma (*2*). The two main nonhereditary

forms of systemic amyloidosis are AA and AL amyloidosis. AA amyloidosis is a major complication of chronic inflammatory diseases such as rheumatoid arthritis and tuberculosis (*3*). The deposits arise from serum amyloid A, an acute-phase protein, present in high concentrations during inflammation (*4*). AL amyloidosis is a complication of plasma cell dyscrasias, such as multiple myeloma or monoclonal gammopathy of undetermined significance. AL deposits consist of monoclonal (κ or λ) immunoglobulin light chains (*5*).

Serum amyloid P component (SAP) has been found in every form of amyloid, independent of the type (*6,7*). It has been shown in vitro to bind to all types of amyloid in a calcium-dependent fashion (*8*). SAP belongs to a group of proteins referred to as pentraxins and consists of a pentameric dimer composed of ten identical subunits with a total molecular weight of approximately 254 kDa (*9*). The physiological function of SAP is as yet unclear, but its plasma concentration appears to be regulated to a constant level in individuals (*10*). Synthesis (*6*) and catabolism (*11*) are confined to the liver (*7*), the plasma half-life is approximately 24 hr (*12*). Amyloid P component is also present outside the circulation, binding to certain components of the extracellular matrix (e.g., elastin microfibrils, proteoglycans, glomerular basement membrane) (*13–15*).

Histological proof is the gold standard for the diagnosis of amyloidosis (*1*). However, sampling errors, the invasive nature of biopsy procedures and the required pathological experience are hampering its use for diagnostic evaluation. For these reasons and the insidious onset of the disease, amyloidosis frequently remains undetected for a long time. Recent observations have shown that amyloidosis may recede after intensive treatment aimed at the elimination of precursor production (*16–18*). Therefore, a noninvasive method for diagnosing amyloidosis and monitoring the effect of treatment would be a helpful clinical tool.

The concept of using radiolabeled SAP as tracer for amyloidosis deposits was developed by the group of Pepys and Hawkins (*19,20*). They found scintigraphy and kinetic studies using radiolabeled SAP to be helpful in diagnosing and localizing amyloidosis (*21*) as well as for monitoring treatment (*22*). The three basic principles of detecting amyloidosis by means of ^{123}I-SAP-studies are: (a) rapid disappearance from the circulation caused by binding to extracellular amyloid deposits resulting in (b) high total-body retention and (c) accurate localization of amyloid deposits.

In this article, we describe ^{123}I-SAP metabolism in a control group and in patients with AA and AL amyloidosis using plasma disappearance rates, retention values and a few derived parameters. We addressed the following questions: are there

TABLE 1
Patient Characteristics

Parameter	Controls	AA	AL
Number	7	25	24
Sex			
Female	2	19	8
Male	5	6	16
Age			
Mean (yr)	50	56	61
Range	25–72	13–74	47–75
Associated disease	3 RA	16 RA	7 Multiple Myeloma
	1 JCA	4 JCA	13 MGUS
	1 MGUS	1 Ankyl Sp	2 Idiopathic
	2 None	1 Psor Artr	1 Waldenstrom
		1 Inf burns	1 NHL
		1 FMF	
		1 Rec pulm inf	
Creat clear (mean, ml/min)	74	47	70
range	46–131	7–107	13–190
Clinical score (mean, points)	2	4	8
range	0–5	1–7	1–13

AA = AA amyloidosis patients; AL = AL amyloidosis patients; RA = rheumatoid arthritis; JCA = juvenile chronic arthritis; MGUS = monoclonal gammopathy of undetermined significance; Psor Artr = psoriatic arthritis; Ankyl Sp = spondylitis ankylopoetica; Inf burns = infected burns; Rec pulm inf = recurrent pulmonary infections; FMF =familiar mediterranean fever; NHL = non-Hodgkin's lymphoma; Creat clear = endogenous creatinine clearance; Clinical score: see text.

differences in these metabolic parameters, and are these related to the type and the amount of amyloid present? The imaging aspects of ^{123}I-SAP scintigraphy in amyloidosis were also analyzed in this study but will be reported separately.

MATERIALS AND METHODS

Patients

Fifty-six people were studied: a control group of 7 with repeatedly negative biopsies and no clinical or laboratory evidence of amyloidosis during the past years, 25 consecutive patients with AA amyloidosis and 24 consecutive patients with AL amyloidosis. All patients had histological proof of systemic amyloidosis. (Multiple positive biopsies taken from subcutaneous fat tissue, liver, kidney, gastrointestinal tract, myocardium, bone marrow, nerve tissue etc.). Patient characteristics are presented in Table 1.

After their SAP study, all patients were studied prospectively for at least 6 mo. Maximum follow-up was 6 yr. At the end of the study period, 20 patients had died (8 AA and 12 AL patients), and 29 patients were still alive (median 27 mo, range 6–79 mo).

The study was approved by the local Ethics Committee and all patients gave informed consent.

Radiolabeling and Quality Control

Highly purified human SAP was kindly supplied by Dr. P.N. Hawkins and Prof. M.B. Pepys. Radiolabeling with ^{123}I (t½ =13.2 hr, obtained from Amersham Cygne, Eindhoven, The Netherlands) was performed according to the method described by Mather and Ward (23). Iodine-123-SAP was purified by gel-filtration chromatography using a sterile PD-10 column (Pharmacia, Woerden, The Netherlands). The protein-containing fractions were pooled and transferred to a sterile vial through a 0.22-μm Millex GV filter (Millipore®, SA, Molsheim, France). Samples were demonstrated to be sterile and pyrogen-free. The TCA-precipitable fraction of the solution was >95%. Calcium-dependent binding to agarose beads (24,25) was >90%, indicating functional integrity of ^{123}I-SAP.

Administration and Sampling

A precisely known dose of 150–200 MBq ^{123}I-SAP containing 100 μg protein [effective dose equivalent reported approximately 4 mSv (20)] was given as an intravenous bolus. Venous plasma samples were drawn from the contralateral arm 15, 30 and 60 min and at 2, 4, 6, 24 and 48 hr after injection. In the first five patients, samples up to 6 days after administration were obtained. Urine was collected for the first and second 24 hr after administration. Thyroid uptake of free iodide was prevented by oral administration of potassium iodide (100 mg daily) from 2 days before to 3 days after injection.

One milliliter of each plasma sample and 2 ml of the urine portions were counted together with an aliquot of the injected material using a gamma counter (Compugamma, LKB Wallac, Finland). The protein-bound fraction in each sample was determined by TCA precipitation. SAP plasma levels were measured by enzyme-linked immunosorbent assay (ELISA). In this sandwich ELISA, a monoclonal anti-SAP (Novocastra Laboratories, Newcastle on Tyne, United Kingdom) was used as a catching antibody and a polyclonal anti-SAP (Dakopatts, Glostrup, Denmark) as a detection antibody. SAP purified from pooled human ascites (provided by P.N. Hawkins) was used as a standard for the assay. The intra-assay variation was 5%, whereas the interassay variation was 8%. The lower detection limit was 15 pg/ml. Reference values were obtained from 50 healthy control subjects: mean SAP levels 26.4 mg/l with a range of 10–48 mg/l.

Analysis of Iodine-123-SAP Clearance

Time-activity curves were constructed from the TCA-precipitable radioactivity. Therefore, the presence of nonprotein-bound radioactivity (e.g., free iodide) did not interfere with the SAP clearance determination. All individual complete plasma disappearance curves were analyzed using fits to a monoexponential, biexponential and tri-exponential function in the first 20 patients. Goodness-of-fit and inter-relations between fitted parameters were compared for these functions using variation coefficients and cross-correlation coefficients for the fitted parameters, the F-ratio test, the linear correlation coefficient between observed and fitted values and Akaike's information criterion. From the use of these criteria, biexponential functions yielded the statistically best fits and were chosen to analyze all further plasma-activity data.

Relative variation coefficients for these biexponential fits were: 10.8% (mean, range 6%–20%) for parameter a, 8.3% (range 2%–17%) for parameter b, 22.6% (range 14%–44%) for parameter m1 and 23.1% (range 6%–45%) for parameter m2 (Fig. 1). Cross-correlation coefficients were generally under 0.50. Linear correlation coefficients were over 0.98 in all cases.

In the first five subjects, plasma samples up to 6 days confirmed the exponential behavior of the terminal clearance phase. Because data from the literature also supported this finding, we stopped sampling at 48 hr p.i (12).

All fits were produced by a computer fitting routine using the Marquardt-Levenberg algorithm (least squares minimization after logarithmic transformation, assuming a constant relative error).

The chosen biexponential function corresponds to a two-compartment model with a central (plasma) compartment and a second reversible compartment (26). Plasma radioactivity can thus be described by the weighted sum of two exponential functions consisting of an initial rapid component and a second slower component (Fig. 1). The initial fast clearance represents equilibration with the reversible compartment; the second component reflects catabolism and disappearance from the circulation. The two components of the curve are characterized each by their half-time and relative fraction. The extrapolated t = 0 value was set to 100% of the injected dose. The plasma samples were thus
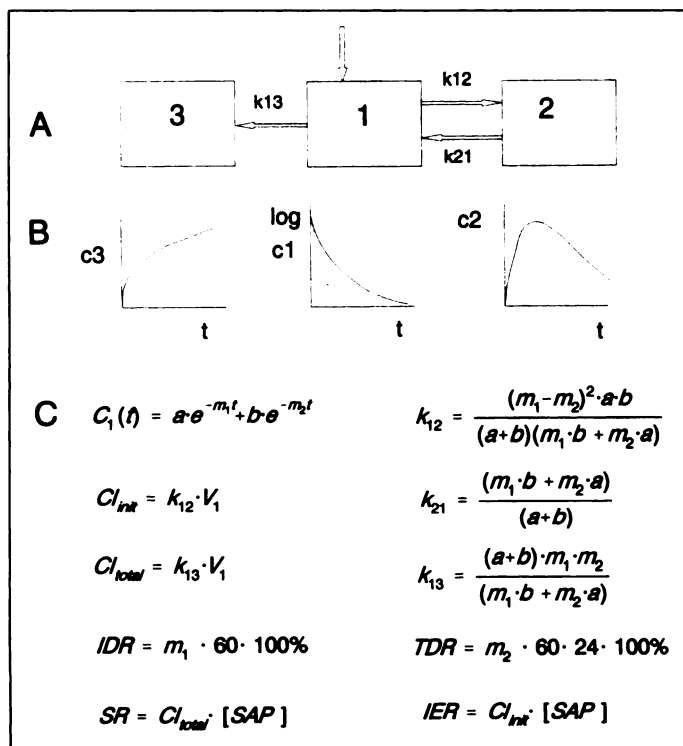
FIGURE 1. Two-compartment model, time-concentration curves and formulas for ^{123}I-SAP metabolism. (A) Injection in central plasma compartment 1. The rate constants are k12, k21, k13. (B) Time-concentration (time-activity) curves; ci = concentration in compartment i. (C) m_1, m_2, a, b = parameters of the corresponding biexponential function, obtained by curve fitting. $C_1(t)$ = concentration in compartment 1 (cpm/ml); Cl_{int} = initial clearance from compartment 1–2 (ml/min); Cl_{total} = total clearance (ml/min); V_1 = Volume of compartment 1 (ml); IDR = initial disappearance rate (%/hr); TDR = total disappearance rate (%/24 hr); SR = synthesis rate (mg/hr); IER = interstitial exchange rate (mg/hr); [SAP]= SAP plasma level (mg/ml).

Figure C equations:

$$C_1(t) = a\cdot e^{-m_1 t} + b\cdot e^{-m_2 t}$$

$$k_{12} = \frac{(m_1-m_2)^2\cdot a\cdot b}{(a+b)(m_1\cdot b + m_2\cdot a)}$$

$$Cl_{int} = k_{12}\cdot V_1$$

$$k_{21} = \frac{(m_1\cdot b + m_2\cdot a)}{(a+b)}$$

$$Cl_{total} = k_{13}\cdot V_1$$

$$k_{13} = \frac{(a+b)\cdot m_1\cdot m_2}{(m_1\cdot b + m_2\cdot a)}$$

$$IDR = m_1 \cdot 60 \cdot 100\%$$

$$TDR = m_2 \cdot 60 \cdot 24 \cdot 100\%$$

$$SR = Cl_{total}\cdot [SAP]$$

$$IER = Cl_{int}\cdot [SAP]$$

expressed as a percentage of the injected dose. Individual values were subsequently averaged per group.

The initial clearance, total clearance, initial disappearance rate and total disappearance rate of ^{123}I-SAP were determined from the two-compartment modeling theory (Fig. 1). Because it can be assumed that SAP metabolism is in steady-state during the 48 hr procedure, the amount of SAP that disappears from the body is equal to the amount that is produced in the body: the synthesis rate of SAP (expressed in mg/hr). The SAP interstitial exchange rate was derived from the initial clearance from compartment 1 into 2 and the total cold SAP plasma concentration (Fig. 1).

Gamma Camera Measurements and Total-Body Retention

Within 10–30 min after injection and after 4, 24 and 48 hr, an anterior and posterior total-body scan and spot views were acquired on a large field of view rectangular gamma camera (Siemens DIACAM or Multispect 2, Hoffman Estates, IL) equipped in the first 12 patients with a low-energy, all-purpose collimator and later with a medium-energy, all-purpose collimator. All four scans in one patient were acquired using the same collimator, and no difference in the relative retention values was found after the collimator transition.

The geometric mean of the total counts in the anterior and posterior total-body scans (background-corrected) shortly after the injection was set to 100%. The background- and decay-corrected geometric means of the later scans were expressed as a percentage of this initial value. No attenuation correction was performed. The total-body retention was also calculated by determining the urine radioactivity expressed as a percentage of the injected dose, as there is no significant extrarenal excretion (12). All urinary activity

was TCA-soluble, even when severe proteinuria was present. In principle, the retention values determined by the urinary excretion method were used for all calculations. The gamma camera derived retention values were used as a measure of quality control of the urine collection. When the difference between the two methods of retention calculation was greater than 10% and when doubts or proven errors regarding adequate urine collection were present, the gamma camera derived values were used instead. The two methods were compared to determine whether camera derived values were equally reliable.

The extravascular retention was determined by subtracting the total-plasma radioactivity, expressed as a percentage of the injected dose, from the total-body retention given by the gamma camera or urine data.

Clinical Estimation of Amyloid Load

A scoring system grading organ involvement was developed in which both organ size and organ function were represented. For each of five categories (heart, kidneys, liver, spleen and all other organs together) a maximum score of four points is possible. For the heart: heart failure = 1 point, left ventricular wall thickness >12 mm = 1 point; low voltage on electrocardiogram = 1 point; left ventricular wall >15 mm = 2 points. For the kidneys: proteinuria >0.25 g/day = 1 point; proteinuria >3.5 g/day = 2 points; endogenous creatinine clearance (ECC) <60 ml/min = 1 point; ECC <30 ml/min = 2 points. For the spleen: enlargement (palpable) = 2 points; Howell Jolly bodies = 2 points. For the liver: enlargement (liver span >15 cm) = 2 points; alkaline phosphatase >200 units/liter = 1 point; alkaline phosphatase >500 units/liter = 2 points. Other organs: clinical dysfunction of gastrointestinal tract (motility disorders, malabsorption); adrenals, thyroid or joints, enlargement of tongue, carpal tunnel syndrome, neuropathy, sicca syndrome: all 1 point, with a category maximum of 4. In this way, the maximum score of organ involvement can be 20.

Statistical Analysis

Means and s.d. were calculated for all parameters in the three groups. Kruskall-Wallis' nonparametric one-way-analysis-of-variance (ANOVA) with Bonferroni's multiple comparisons test was used to compare parameters between the three groups. Parametric tests could not be used because the assumption of equal s.d. in the reference populations from which our samples were drawn was not satisfied (validated by Bartlett's test for homogeneity of variances). Correlation coefficients (linear) were parametric or nonparametric as appropriate. Survival analysis was performed using the Kaplan-Meier method for presentation and the log-rank test for comparison of groups. Two-tailed probability (p) values <5% were considered significant.

RESULTS

Iodine-123-SAP plasma disappearance curves were biphasic in the control subjects and in all amyloidosis patients and could adequately be fitted to a weighted biexponential function. In the amyloidosis patients, there was a significantly faster initial plasma disappearance compared to the control subjects, especially in the AL patients. This difference was only present in the initial exponential phase (the first 6 hr) and had disappeared at 24 and 48 hr after injection. Parameters describing plasma disappearance are presented in Figure 2 and Table 2. No difference in plasma kinetics, as represented by total clearance rates, fractional catabolic rates and synthesis rates, was found in the second part of the curves, from 24–48 hr. We observed no differences in SAP plasma levels between the AA amyloidosis patients and control subjects. In AL amyloidosis, plasma SAP
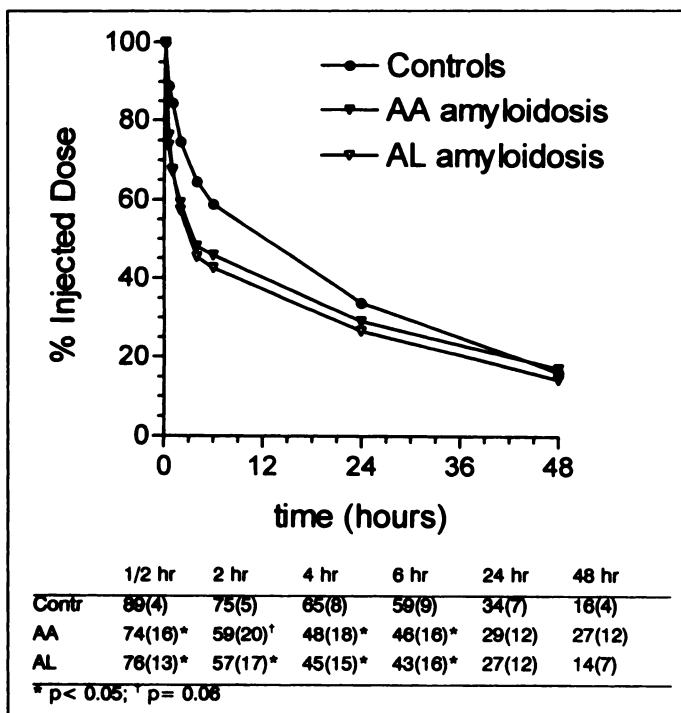
	1/2 hr	2 hr	4 hr	6 hr	24 hr	48 hr
Contr	89(4)	75(5)	65(8)	59(9)	34(7)	16(4)
AA	74(16)*	59(20)†	48(18)*	46(16)*	29(12)	27(12)
AL	76(13)*	57(17)*	45(15)*	43(16)*	27(12)	14(7)

*p< 0.05; † p= 0.06

FIGURE 2. Iodine-123-SAP plasma disappearance curves for the control group (contr) and both amyloidosis groups (AA and AL). Mean values and s.d. Values are group averages of all individually fitted time-activity curves.

tended to be lower, but the difference did not reach statistical significance (Table 2).

Total-body retention was clearly higher in the two amyloidosis groups in comparison with the control subjects at 24 and 48 hr after injection (Table 3). The difference was slightly larger at 48 hr. The gamma camera determined retention values correlated well with the retention as determined from the urinary excretion (Fig. 3). If the difference between the two methods was greater than 10%, errors in urine collection appeared to be the cause in nearly all cases.

The extravascular retention values (total-body retention minus plasma activity) were clearly higher in the amyloidosis patients compared to the control group (Table 3). While in the control subjects the extravascular ^{123}I-SAP retention is decreasing after 24 hr, retention in the amyloidosis patients remained stable. Presumably, this is due to a large proportion of the tracer still binding in the extravascular amyloid deposits. Figure 4 shows a typical example of plasma kinetics and retention values

TABLE 2
Metabolic Data of Iodine-123-SAP: Mean Values (s.d.)

Metabolic parameter	Controls	AA	AL
$T_{1/2}$ initial (min)	66 (24)	52 (42)	49 (27)
relative fraction (%)	30 (11)	48 (19)*	49 (17)*
$T_{1/2}$ total (hr)	23 (4)	34 (22)	28 (10)
relative fraction (%)	70 (11)	52 (19)*	51 (17)*
Initial disapp rate (%/hr)	71 (23)	126 (78)	118 (73)
Total disapp rate (%/24 hr)	74 (11)	58 (21)	68 (27)
Plasma SAP (mg/liter)	32 (7)	34 (11)	25 (13)
Initial clearance (ml/min)	9 (3)	33 (29)*	49 (52)*
Interstitial exchange rate (mg/hr)	18 (8)	64 (61)*	50 (37)*
Total clearance (ml/min)	2.3 (0.5)	2.6 (1.5)	4.7 (4.7)
Synthesis rate (mg/hr)	4.5 (1.4)	5.0 (3.0)	5.5 (3.2)

*p<0.05 for comparison between AA or AL vs. controls.
AA = AA amyloidosis patients; AL = AL amyloidosis patients.

TABLE 3
Iodine-123-SAP Retention Data: Mean Values (s.d.)

	Controls	AA	AL
Urinary excretion method			
Total-body retention 24 hr p.i. (%)	71 (13)	87 (9)†	86 (10)†
Total-body retention 48 hr p.i. (%)	46 (15)	74 (14)‡	73 (17)†
Gamma camera method			
Total-body retention 24 hr p.i. (%)	74 (12)	88 (10)†	86 (12)*
Total-body retention 48 hr p.i. (%)	50 (16)	74 (15)†	70 (19)*
Extravascular retention 24 hr p.i. (%)	37 (11)	58 (15)†	59 (16)‡
Extravascular retention 48 hr p.i. (%)	30 (14)	59 (16)†	58 (19)†

*p<0.05; †p<0.01; ‡p<0.001 for comparison between AA or AL vs. controls.

AA = AA amyloidosis patients; AL =AL amyloidosis patients; disapp = disappearance.

in one of the control subjects and in a patient with extensive AL amyloidosis.

Total-body retention correlated inversely with renal function, reflecting slow excretion of free iodide and other small metabolites in patients with impaired renal function ($r = -0.54$, $p < 0.01$). This was particularly true in the AA amyloidosis group, that had a lower average endogenous creatinine clearance value. The extravascular retention values, however, were less influenced by renal function ($r = -0.35$, $p < 0.01$) (Fig. 5A and 5B). When combining plasma disappearance and extravascular retention most patients are well outside the normal range (Fig. 6).

The clinical amyloid severity score correlated with the extravascular ^{123}I-SAP retention at 48 hr p.i. in amyloidosis patients (Fig. 7A). For the AA amyloidosis patients, we found a correlation coefficient $r = 0.54$ ($p < 0.01$). AL amyloidosis patients had a wider range of scores, in agreement with the higher degree of severity of AL amyloidosis, resulting in a
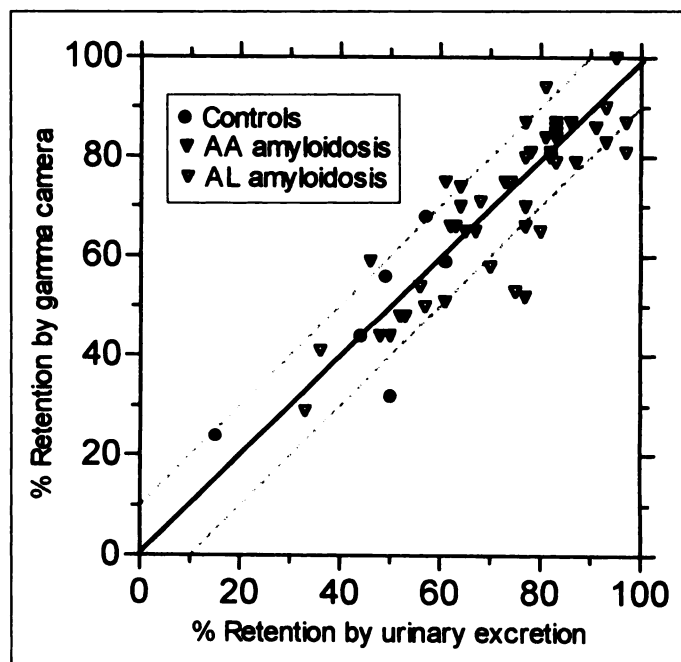

FIGURE 3. Comparison of 48-hr total-body ^{123}I-SAP retention derived from urinary excretion (x-axis) with retention value calculated from gamma camera data (y-axis) for all subjects. The continuous line is the line of identity. Dotted lines represent 10% difference region, the tolerance level. Points outside this region contain errors in urinary sampling.
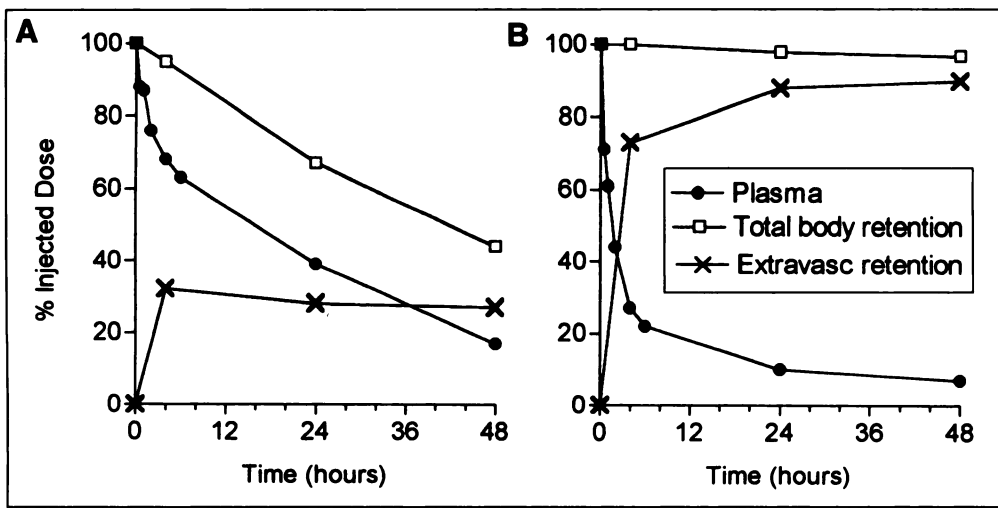
FIGURE 4. Plasma disappearance curve, total-body retention and extravascular retention curve for (A) one of the control subjects and (B) for a severely affected AL amyloidosis patient. In this patient, very rapid plasma disappearance is present as well as very high total-body and extravascular ^{123}I-SAP retention.

correlation coefficient r = 0.67 (p < 0.001) in this group (Fig. 7B).

Thirteen of the 20 patients who died during the study period had more than 60% extravascular ^{123}I-SAP retention at 48 hr. In the patients with AA amyloidosis and retention values of 60% or more no difference in survival was found (Fig. 8A). In patients with AL amyloidosis and retention values of 60% or more, the survival (median 4 mo) differed significantly (p < 0.001) from the survival (median 23 mo) of the patients with retention values below 60% (Fig. 8B).

DISCUSSION

The metabolism of ^{123}I-SAP in patients with amyloidosis shows distinct differences from amyloid-free control subjects. This relatively large protein (SAP) appears to exchange rapidly between plasma and a second compartment, most likely the extracellular space. Although modeling and fitting to any compartment model must be a simplification of the complex reality, such a two-compartment model is suggested by the biexponential shape of the plasma curves with a rapid initial component, and rapid organ uptake as can be visualized on scintigrams (19), the finding of radiolabeled SAP in tissue sections at autopsy (20) and the experience in animal models (27,28). While others report a monoexponential disappearance in normal control subjects and patients (12,29), we observed biexponential disappearance in all subjects, although the relative fraction of the initial exponential component was lower in the control group (Table 2). This is consistent with the fact that SAP is present in conjunction with certain components of the

extracellular matrix also in subjects without amyloidosis (13–15).

Iodine-123-SAP Plasma Clearance

The rapid exchange between plasma and the extracellular compartment is illustrated by the initial SAP clearance from plasma to this second compartment (presumably the interstitium) being enhanced by a factor of 3–4 in amyloidosis. When expressed as interstitial exchange rate in milligrams per hour, this exchange appeared to be over 200 mg/hr in some patients (versus 18 mg/hr in the control subjects) at a plasma SAP level around 30 mg/liter, indicating a very dynamic process.

Plasma SAP levels in the control group were in the same range as reported by others (12,30). There was no difference between the control subjects and the amyloidosis patients, although the level in AL patients tended to be lower. In a few very severely affected AL amyloidosis patients, SAP plasma levels were markedly decreased compatible with terminal failure of liver protein synthesis function.

While the initial SAP clearance and SAP interstitial exchange rate clearly differed between patients and control subjects, we found no difference in total SAP clearance and SAP synthesis rate in the amyloidosis patients compared with the control subjects. This indicates that the high initial binding to amyloid deposits is at least partly reversible. Such a mechanism seems to be more conceivable than assuming irreversible trapping of ^{123}I-SAP in amyloid deposits. This would lead to a highly increased synthesis rate as described by Hawkins et al. (12,19) who found a much increased (30-fold) SAP synthesis rate in
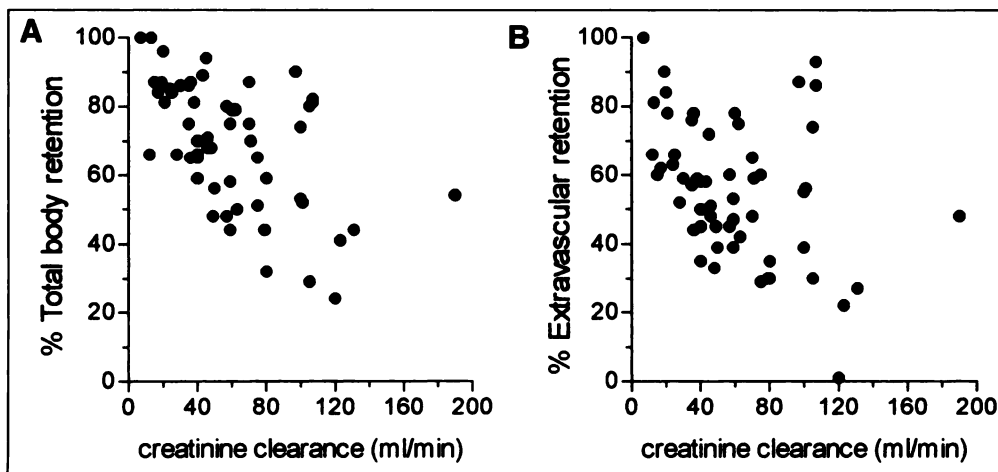

FIGURE 5. (A) Scatterplot for all subjects with endogenous creatinine clearance versus ^{123}I-SAP total-body retention at 48 hr p.i.; r = −0.54, p < 0.01. (B) Scatter plot with creatinine clearance versus extravascular retention at 48 hr p.i.; r = −0.35, p < 0.01.

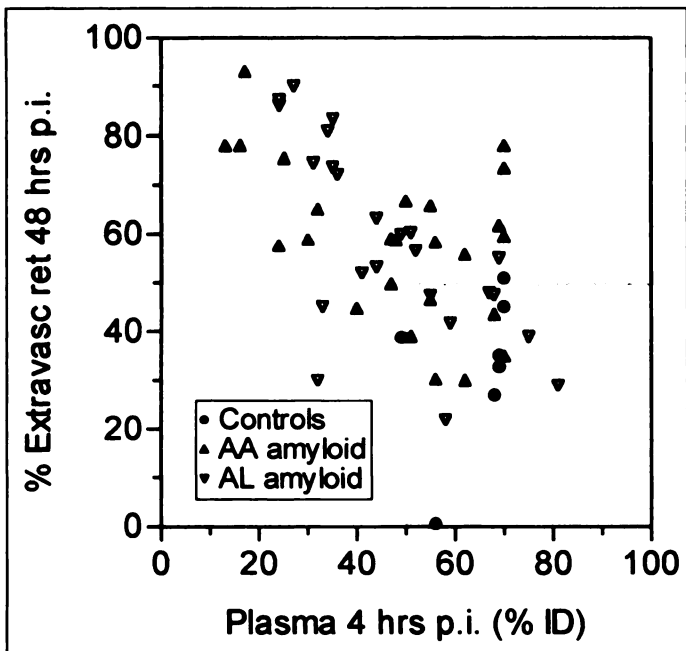**FIGURE 6.** Scatterplot combining ^{123}I-SAP plasma level 4 hr p.i. (x-axis) with ^{123}I-SAP extravascular retention 48 hr p.i. (y-axis). The circumlined area below right contains the observations obtained in the control subjects, "the normal area."

amyloidosis. Their studies were performed using ^{125}I-labeled SAP, permitting prolonged observation. However, with a plasma half-life of approximately 24 hr, it is possible to get a reasonable estimation of the terminal clearance phase using ^{123}I in a 48-hr procedure, as was validated by others and in our first five patients (12). Therefore, the discrepancy cannot be attributed to the longer sampling interval possible when using ^{125}I. Their calculations, however, were performed in only a few patients with extremely large amyloid deposits with probably massive first-pass extraction. In that case, curve fitting procedures, especially to the second exponential phase, might produce unreliable results. Our SAP synthesis rate in the control subjects, however, was slightly higher, but basically in the same range, as previously reported (12).

Reliably expressing very fast ^{123}I-SAP clearance in one parameter is difficult. When extensive amyloid is present, the plasma disappearance can be too fast for adequate venous mixing by first-pass extraction in, for example, the liver or spleen during the first 15 or even 30 min in extreme cases. Back extrapolation to t = 0 in this initial steep part of the curve could
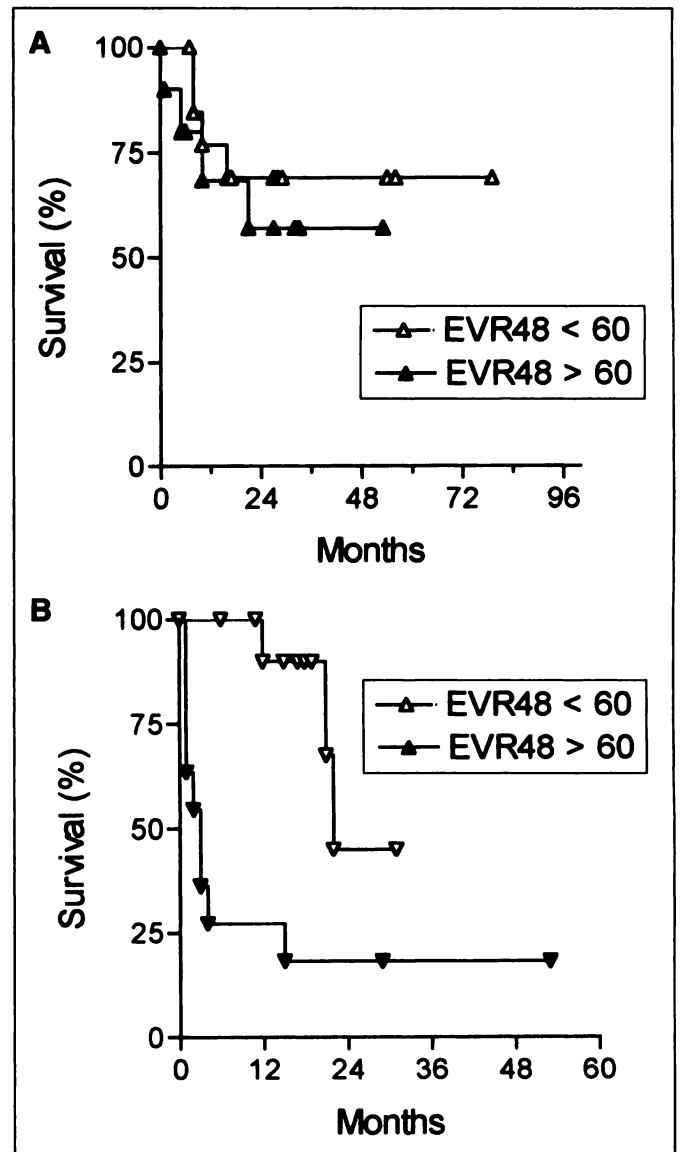

FIGURE 8. Survival curves of patients with extravascular ^{123}I-SAP extravascular retention 48 hr p.i. 60% (closed symbols), and <60% (open symbols). (A) Patients with AA amyloidosis. (B) Patients with AL amyloidosis.

introduce a large error. Expressing plasma retention as a percentage of this t = 0 value and calculation of the initial distribution volume will, therefore, contain the same error. This might be one of the reasons that different authors find different
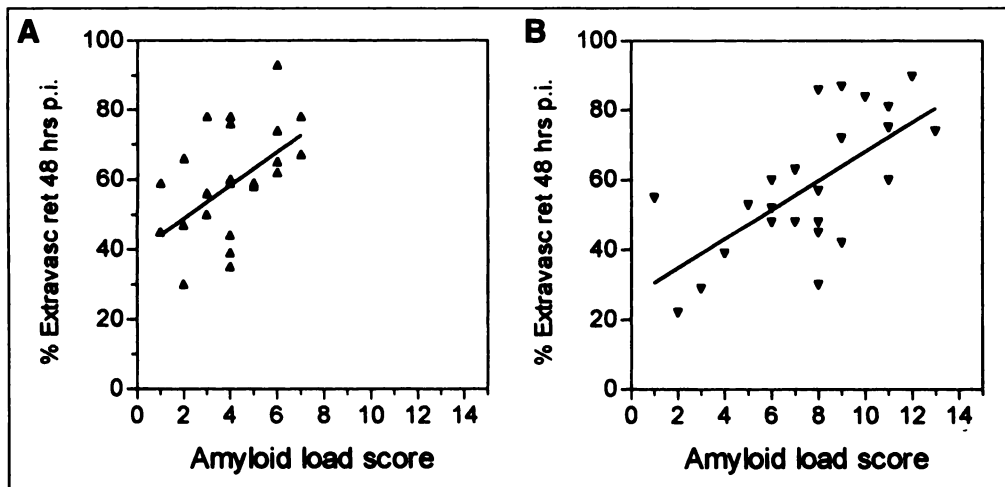

FIGURE 7. Relation between amyloid load score and ^{123}I-SAP extravascular retention at 48 hr p.i. for (A) AA amyloidosis patients (r = 0.54) (p < 0.01), including regression line, and (B) AL amyloidosis patients (r = 0.67) (p < 0.001), including regression line.

6-hr plasma values (20,29,31). Precise calculations of the volume of distribution at t = 0 in severely affected patients should be used with caution for these reasons (29). In normal control subjects and patients with only minor depositions, however, this error is scarcely present.

Despite these difficulties in extreme cases, the 2-, 4- or 6-hr plasma value can serve as a good and simple measure of ^{123}I-SAP disappearance, displaying a clear difference between control subjects and amyloidosis patients although with some overlap. Because amyloid deposition is a gradual and slow process, this overlap probably reflects the transition of no amyloid to clinically relevant amyloid. Others have found less overlap between normal subjects and amyloidosis patients, but this may depend on patient selection and especially the relative number of severe cases included (20,31). In our situation, the study population consisted of consecutive patients with all ranges of severity.

Total-Body Retention

Total-body ^{123}I-SAP retention, which can be considered another measure of the amount of amyloid present, was significantly higher in the amyloidosis patients, and the difference with the control group was already present at 24 hr and especially at 48 hr after injection. We observed no systematic difference in the retention values determined by urinary excretion analysis or gamma camera measurements, which was consistent with the absence of major extrarenal clearance (12). However, total-body retention values are slightly influenced by renal function: in control subjects, 34% of the injected dose is still present as protein-bound radioactivity (SAP) in the plasma at 24 hr postinjection. Because total-body retention at 24 hr was found to be 74%, 40% of the dose is still present in the body in the form of ^{123}I-SAP, free [123]Iodide or [123]Iodo-amino-acid residues in tissues. This is more than expected from the fractional catabolic rate (74%/24 hr) and, therefore, there must be some delay in excreting the metabolites. Also, because iodide clearance in normal renal function is on the order of 30 ml/min (32) and SAP clearance generally around 3–4 ml/min it can be expected that in severe renal dysfunction the free iodide clearance will approach the SAP clearance. The assumption that elimination of SAP metabolites by the kidney is so fast that its influence on the retention can be neglected (12,19,20) needs modification. In severely impaired renal function, this results in a too high total-body retention. This occurred especially in the AA amyloidosis group in which renal function is frequently impaired (Fig. 5A). The analysis of plasma disappearance, however, is not affected by the impaired clearance of free iodide, because only TCA precipitable radioactivity was analyzed.

Extravascular retention values were less troubled by this effect, probably because subtracting plasma activity partly corrects for renal function abnormalities (Fig. 5B). Saile et al. also found extravascular retention to be a quite sensitive parameter for grading amyloidosis (31). Their determination of plasma activity, however, was only based on three samples and an estimation of plasma volume instead of analyzing a complete curve. Hawkins et al. found extravascular retention values in the same range as in this study (12). Zingraff et al. also concluded extravascular distribution to be a sensitive parameter for the presence of amyloidosis, although in a different population of (dialysis associated β2-microglobulin) amyloidosis patients (29).

Clinical Value

Our clinical amyloid load score, although only an estimation, correlated with the 48-hr extravascular retention (Fig. 7). In patients with AL amyloidosis, high extravascular ^{123}I-SAP retention of 60% or more was associated with shorter survival, as also observed elsewhere (33). This effect was not seen in patients with AA amyloidosis, possibly because in AA amyloidosis disease progression is generally much slower and fewer vital organs are affected compared to AL amyloidosis requiring a longer follow up than in this study.

Based on the observations in the control group, we used 50% as a cutoff value between normal subjects and patients (2 s.d. from the mean), both for the 4-hr plasma value and the 48-hr extravascular retention parameter. By using this 50–50 criterion, we calculated a sensitivity for the detection of amyloidosis of 73% at a specificity of 100% for the 4-hr plasma value and the 48 hr extravascular retention parameters together (Fig. 6). By using a cutoff value of 55% for the 4-hr plasma value and 45% for the 48-hr extravascular retention, sensitivity rises to 84%, but specificity decreases to 71%.

These parameters can serve as clinical tools for evaluation of amyloidosis patients. A quantitative impression of the amount of amyloid present is almost impossible to get using other procedures during life. Even multiple biopsies from many organs provide only a qualitative idea of the amount of amyloidosis and serial monitoring is not possible.

Proposed ^{123}I-SAP Behavior in Vivo

After injection, ^{123}I-SAP rapidly equilibrates between the plasma and the extravascular space with possible interactions with basement membranes, proteoglycans (15), fibronectin (34) and type IV collagen (35). However, if amyloid is present, SAP binds avidly and, to a large extent, reversibly to amyloid. This occurs especially where close contact exists between plasma and the extravascular matrix as in the liver, spleen and bone marrow. Therefore, the disappearance rate of ^{123}I-SAP from the circulation depends on the amount as well as the accessibility of the amyloid deposits. Consequently, it is not likely to find early ^{123}I-SAP uptake (i.e., within 48 hr) in organs with a nonaccessible amyloid pool (e.g., myocardium, brain), as has indeed been observed in imaging studies, whereas amyloid deposits in liver, spleen and kidneys are easier to visualize (19–21). Imaging of Alzheimer's disease associated amyloid deposits is, therefore, highly unlikely within days after ^{123}I-SAP injection.

Because the SAP synthesis rate appears to be rather constant, the increased quantity of SAP present in amyloidosis must be caused by an only slightly elevated synthesis rate present for a long time. In the extravascular pool, part of the SAP might become irreversibly trapped in deeper amyloid layers that are not prone to backdiffusion to the circulation anymore.

CONCLUSION

There are striking differences in ^{123}I-SAP metabolism between amyloidosis patients and normal control subjects. Like others, we found a faster initial disappearance from the plasma, a higher total-body retention and, especially, a higher extravascular retention. Retention values could reliably be determined with a gamma camera. While markedly increased interstitial exchange rates were present in amyloidosis, we observed no difference in SAP synthesis rates in these patients compared with the control subjects. Patients with AA and AL amyloidosis did not differ from each other in this respect.

In combination with total-body scintigraphy, these data are of clinical use in supporting the diagnosis, establishing the gravity of the disease, determining prognosis and probably monitoring treatment. The results of 2-, 4- or 6-hr plasma retention values, total-body and, especially, extravascular retention values are presumably good measures of the total-body amyloid burden.

This nuclear medicine procedure might be the only method to provide this information during life, although the overlap between normal control subjects and patients with minimal amyloid depositions might make this method less suitable for screening purposes.

REFERENCES

1. Van der Hem GK, van Rijswijk MH. Amyloidosis. In: Cameron S, Davidson AM, Grünfeld J-P, et al., eds. *Oxford textbook of clinical nephrology*, 2nd ed. Oxford: Oxford University Press; 1992:545–561.
2. Husby G. Classification of amyloidosis. In: Husby G, ed. *Reactive amyloidosis and the acute phase response. Baillière's clinical rheumatology*. London: Baillière Tindall; 1994:503–511.
3. Hazenberg BPC, van Rijswijk MH. Clinical and therapeutic aspects of AA amyloidosis. In: Husby G, ed. *Reactive amyloidosis and the acute phase response. Baillière's clinical rheumatology*. London: Baillière Tindall; 1994:661–690.
4. Husby G, Marhaug G, Dowton B, Sletten K, Sipe JD. Serum amyloid A (SAA): biochemistry, genetics and the pathogenesis of AA amyloidosis. *Amyloid: Int J Clin Invest* 1994;1:119–137.
5. Solomon A, Weiss DT. Protein and host factors implicated in the pathogenesis of light chain amyloidosis (AL amyloidosis). *Amyloid: Int J Clin Invest* 1995;2:269–279.
6. Pepys MB, Baltz ML, de Beer FC, et al. Biology of serum amyloid P component. *Ann NY Acad Sci* 1982;389:286–297.
7. Pepys MB, Rademacher TW, Amatayakul-Chantler S, et al. Human serum amyloid P component is an invariant constituent of amyloid deposits and has a uniquely homogeneous glycostructure. *Proc Natl Acad Sci USA* 1994;91:5602–5606.
8. Pepys MB, Dyck RF, de Beer FC, Skinner M, Cohen AS. Binding of serum amyloid P-component (SAP) by amyloid fibrils. *Clin Exp Immunol* 1979;38:284–293.
9. Pepys MB, Baltz ML. Acute phase proteins with special reference to C-reactive protein and related proteins (pentraxins) and serum amyloid A protein. *Adv Immunol* 1983;34:141–211.
10. Pepys MB, Dash AC, Makham RE, Thomas HC, Williams BD, Petrie A. Comparative clinical study of protein SAP (amyloid P component) and C-reactive protein in serum. *Clin Exp Immunol* 1978;32:119–124.
11. Hutchinson WL, Noble GE, Hawkins PN, Pepys MB. The pentraxins, C-reactive protein and serum amyloid P component, are cleared and catabolized by hepatocyes in vivo. *J Clin Invest* 1994;94:1390–1396.
12. Hawkins PN, Wootton R, Pepys MB. Metabolic studies of radioiodinated serum amyloid P component in normal subjects and patients with systemic amyloidosis. *J Clin Invest* 1990;86:1862–1869.
13. Dyck RF, Lockwood CM, Kershaw M, et al. Amyloid P-component is a constituent of normal human glomerular basement membrane. *J Exp Med* 1980;152:1162–1174.
14. Breathnach SM, Melrose SM, Bhogal B, et al. Amyloid P component is located on elastic fibre microfibrils in normal human tissue. *Nature* 1981;293:652–653.
15. Hamazaki H. Ca^{2+}-mediated association of human serum amyloid P component with heparan sulfate and dermatan sulfate. *J Biol Chem* 1987;262:1456–1460.
16. Perfetti V, Bellotti V, Maggi A, et al. Reversal of nephrotic syndrome due to reactive amyloidosis (AA-type) after excision of localized Castleman's disease. *Am J Hematol* 1994;46:189–193.
17. Suhr OB, Holmgren G, Steen L, et al. Liver transplantation in familial amyloidotic polyneuropathy: follow-up of the first 20 Swedish patients. *Transplantation* 1995;60:933–938.
18. Moreau P, Milpied N, de Faucal P, et al. High-dose melphalan and autologous bone marrow transplantation for systemic AL amyloidosis with cardiac involvement. *Blood* 1996;87:3063–3064.
19. Hawkins PN, Myers MJ, Lavender JP, Pepys MB. Diagnostic radionuclide imaging of amyloid: biological targeting by circulating human serum amyloid P component. *Lancet* 1988;i:1413–1418.
20. Hawkins PN, Lavender JP, Pepys MB. Evaluation of systemic amyloidosis by scintigraphy with ^{123}I-labeled serum amyloid P component. *N Engl J Med* 1990;323:508–513.
21. Hawkins PN, Richardson S, MacSweeney JE, et al. Scintigraphic quantification and serial monitoring of human visceral amyloid deposits provide evidence for turnover and regression. *Q J Med* 1993;86:365–374.
22. Hawkins PN, Richardson S, Vigushin DM, et al. Serum amyloid P component scintigraphy and turnover studies for diagnosis and quantitative monitoring of AA amyloidosis in juvenile rheumatoid arthritis. *Arth Rheum* 1993;36:842–851.
23. Mather SJ, Ward BC. High efficiency iodination of monoclonal antibodies for radiotherapy. *J Nucl Med* 1987;28:1034–1036.
24. De Beer FC, Pepys MB. Isolation of human C-reactive protein and serum amyloid P component. *J Immunol Methods* 1982;50:17–31.
25. Hind CRK, Collins PM, Renn D, et al. Binding specificity of serum amyloid P component for the pyruvate acetyl of galactose. *J Exp Med* 1984;159:1058–1069.
26. Gibaldi M, Perrier D. Multicompartment models. In: Gibaldi M, Perrier D. *Pharmacokinetics*, first edition. New York: Dekker; 1975:45–88.
27. Baltz ML, Caspi D, Evans DJ, Rowe IF, Hind CRK, Pepys MB. Circulating serum amyloid P component is the precursor of amyloid P component in tissue amyloid deposits. *Clin Exp Immunol* 1986;66:691–700.
28. Caspi D, Zalzman S, Baratz M, et al. Imaging of experimental amyloidosis with ^{131}I-labelled serum amyloid P component. *Arth Rheum* 1987;30:1303–1306.
29. Zingraff J, Caillat-Vigneron N, Ureña P, et al. Plasma kinetics of ^{125}I-labeled amyloid P component in β2M amyloidosis: a possible approach to quantitate disease activity. *Nephrol Dial Transplant* 1995;10:223–229.
30. Skinner M, Vaitukaitis JL, Cohen AS, Benson MD. Serum amyloid P-component levels in amyloidosis, connective tissue diseases, infection and malignancy as compared to normal serum. *J Lab Clin Med* 1979;97:633–638.
31. Saïle R, Deveaux M, Hachulla E, Descamps J, Duquesnoy B, Marchandise X. Iodine-123-labeled serum amyloid P component scintigraphy in amyloidosis. *Eur J Nucl Med* 1993;20:130–137.
32. Koutras DA, Marketos SG, Rigopoulos GA, Malamos B. Iodine metabolism in chronic renal insufficiency. *Nephron* 1972;9:55–65.
33. Hachulla E, Maulin L, Deveaux M, et al. Prospective and serial study of primary amyloidosis with serum amyloid P component scintigraphy: from diagnosis to prognosis. *Am J Med* 1996;101:77–87.
34. Kawahara E, Shiroo M, Nakanishi I, Migita S. The role of fibronectin in the development of experimental amyloidosis–evidence of immunohistochemical codistribution and binding property with serum amyloid protein-A. *Am J Pathol* 1989;134:1305–1314.
35. Zahedi K. Characterization of the binding of serum amyloid P to type IV collagen. *J Biol Chem* 1996;271:14897–14902.